

# ***N*-Methyl-*N*-((1-methyl-5-(3-(1-(2-methylbenzyl)piperidin-4-yl)propoxy)-1*H*-indol-2-yl)methyl)prop-2-yn-1-amine, a New Cholinesterase and Monoamine Oxidase Dual Inhibitor**

Oscar M. Bautista-Aguilera,<sup>†</sup> Abdelouahid Samadi,<sup>†</sup> Mourad Chioua,<sup>†</sup> Katarina Nikolic,<sup>‡</sup> Slavica Filipic,<sup>‡</sup> Danica Agbaba,<sup>‡</sup> Elena Soriano,<sup>§</sup> Lucía de Andrés,<sup>||</sup> María Isabel Rodríguez-Franco,<sup>||</sup> Stefano Alcaro,<sup>⊥</sup> Rona R. Ramsay,<sup>#</sup> Francesco Ortuso,<sup>\*,⊥</sup> Matilde Yañez,<sup>\*,∇</sup> and José Marco-Contelles<sup>\*,†</sup>

<sup>†</sup>Laboratorio de Química Médica, (IQOG, CSIC), Juan de la Cierva 3, E-28006 Madrid, Spain

<sup>‡</sup>Institute of Pharmaceutical Chemistry, Faculty of Pharmacy, University of Belgrade, Vojvode Stepe 450, 11000 Belgrade, Serbia

<sup>§</sup>SEPCO, (IQOG, CSIC), Juan de la Cierva 3, 28006 Madrid, Spain

<sup>||</sup>Instituto de Química Médica, (IQM-CSIC), C/Juan de la Cierva 3, 28006 Madrid, Spain

<sup>⊥</sup>Dipartimento di Scienze della Salute, Università "Magna Græcia" di Catanzaro, Campus "S. Venuta", Viale Europa, 88100 Catanzaro, Italy

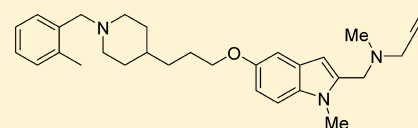
<sup>#</sup>Biomedical Sciences Research Complex, University of St Andrews, Biomolecular Sciences Building, North Haugh, St Andrews KY16 9ST, U.K.

<sup>∇</sup>Facultad de Farmacia, Departamento de Farmacología, Universidad de Santiago de Compostela, Campus Vida, La Coruña, 15782 Santiago de Compostela, Spain

## **S Supporting Information**

**ABSTRACT:** On the basis of *N*-((5-(3-(1-benzylpiperidin-4-yl)propoxy)-1-methyl-1*H*-indol-2-yl)methyl)-*N*-methylprop-2-yn-1-amine (**II**, ASS234) and QSAR predictions, in this work we have designed, synthesized, and evaluated a number of new indole derivatives from which we have identified *N*-methyl-*N*-((1-methyl-5-(3-(1-(2-methylbenzyl)piperidin-4-yl)propoxy)-1*H*-indol-2-yl)methyl)prop-2-yn-1-amine (**2**, MBA236) as a new cholinesterase and monoamine oxidase dual inhibitor.

## **A New Cholinesterase and Monoamine Oxidase Dual Inhibitor**



*N*-Methyl-*N*-((1-methyl-5-(3-(1-(2-methylbenzyl)piperidin-4-yl)propoxy)-1*H*-indol-2-yl)methyl)prop-2-yn-1-amine (**2**, MBA236)

IC <sub>50</sub> (hMAO-A)	IC <sub>50</sub> (hMAO-B)	IC <sub>50</sub> (hAChE)	IC <sub>50</sub> (hBuChE)
6.3 ± 0.4 nM	183.6 ± 7.4 nM	2.8 ± 0.1 μM	4.9 ± 0.2 μM

## **■ INTRODUCTION**

Alzheimer's disease (AD) is an age-related neurodegenerative disorder that accounts for approximately 70% of adult dementia.<sup>1</sup> Worldwide, it is estimated that 40 million people suffer from AD, and the prevalence of AD is expected to rise significantly in the next decades, as the average age of the population increases.<sup>2</sup> AD is characterized by a progressive memory loss and a decline in language skills and other cognitive impairments.<sup>3</sup> Although the etiology of AD is not completely known, common hallmarks, such as amyloid- $\beta$  (A $\beta$ )<sup>4</sup> deposits,  $\tau$ -protein aggregation,<sup>5</sup> and oxidative stress,<sup>6</sup> are thought to play key roles in the pathophysiology of the disease.<sup>7</sup> In addition, the selective loss of cholinergic neurons in AD results in a deficit of acetylcholine (ACh) in specific brain regions that mediate learning and memory.<sup>8</sup> However, alterations in other neurotransmitter systems, specially serotonergic and dopaminergic, are also thought to be

responsible for the behavioral disturbances observed in AD patients.<sup>9</sup>

Monoamine oxidase (MAO; EC1.4.3.4), the enzyme that catalyzes the oxidative deamination of a variety of biogenic and xenobiotic amines,<sup>10</sup> is also an important target to be considered for the treatment of specific features of AD. MAO exists as two distinct enzymatic isoforms, MAO-A and MAO-B, based on their substrate and inhibitor specificities.<sup>11</sup> MAO-A preferentially deaminates serotonin, adrenaline, and noradrenaline and is selectively and irreversibly inhibited by clorgyline. In contrast, MAO-B preferentially deaminates  $\beta$ -phenylethylamine and benzylamine and is irreversibly inhibited by L-deprenyl.<sup>12</sup> Selective inhibitors for MAO-A are effective antidepressants, whereas MAO-B inhibitors are useful in the treatment of Parkinson's disease (PD)<sup>13</sup> and might also be valuable for the

**Received:** September 18, 2014

**Published:** November 24, 2014

treatment of AD.<sup>14</sup> In fact, MAO-B inhibitors are also currently in clinical trials for the treatment of AD because an increased level of MAO-B has been detected in the plaque-associated astrocytes of brains from AD patients.<sup>15</sup>

At present, there are three FDA-approved drugs (donepezil, galantamine, and rivastigmine)<sup>16,17</sup> that improve AD symptoms by inhibiting acetylcholinesterase (AChE; EC1.1.1.7), i.e., the enzyme responsible for the hydrolysis of ACh, and thereby raising ACh content in the synapsis. Apart from the beneficial palliative properties of AChE inhibitors in AD,<sup>18,19</sup> cholinergic drugs have shown little efficacy to prevent the progression of the disease. Consequently, there is no efficient therapy to cure, stop, or even slow the progression of the disease; therefore, effective therapeutics are urgently sought and needed.

The failure to find such a drug or treatment is possibly due to the multifactorial nature of AD. Thus, a single drug that acts on a specific target to produce the desired clinical effects might not be suitable for the complex nature of AD. Accordingly, the multitarget-directed ligand (MTDL) approach<sup>20–22</sup> has been the subject of increasing attention by many research groups, which have developed a variety of compounds acting on very diverse targets.<sup>23–26</sup>

We have previously reported *N*-((5-(benzyloxy)-1*H*-indol-2-yl)methyl)prop-2-yn-1-amine (I, PF9601N)<sup>27</sup> (Figure 1) as a

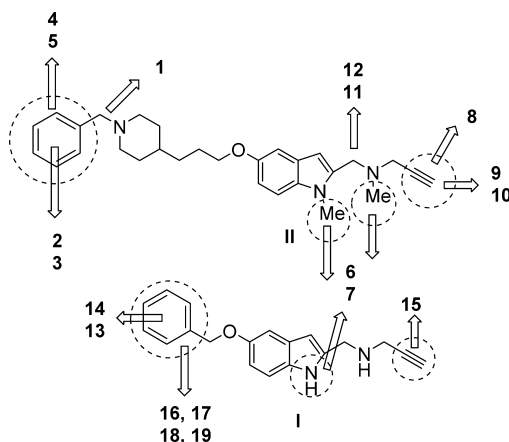


**Figure 1.** Schematic structural and functional modifications in compounds I and II leading to the new target molecules 1–19.

potent and selective propargylamine-containing MAO-B inhibitor (MAOBI) possessing neuroprotective properties that, unlike *L*-deprenyl does not generate amphetamines when metabolized and possesses antiapoptotic properties.<sup>28</sup> Next we used I as *hit* compound with therapeutic potential for the treatment of neurodegenerative diseases and started a project targeted to finding an improved *lead* compound.

As a result of this effort, we found that *N*-((5-(3-(1-benzylpiperidin-4-yl)propoxy)-1-methyl-1*H*-indol-2-yl)methyl)-*N*-methylprop-2-yn-1-amine (II, ASS234, Figure 1) is a multipotent drug able to inhibit human AChE (hAChE) and human butyrylcholinesterase (hBuChE), showing inhibition of human MAO-A and human MAO-B (hMAO-A, hMAO-B).<sup>29</sup> The kinetic analysis demonstrated that compound II is not only a reversible inhibitor of both hAChE and hBuChE with micromolar affinity but a highly potent irreversible inhibitor of hMAO-A, similarly to clorgyline.<sup>30</sup> The crystal structure of human MAO-B in complex with compound II highlighted the covalent adduct formed with the flavin N5 atom, which, based

on the spectral changes, occurs also with the MAO-A cofactor.<sup>30</sup> Hybrid II inhibited  $A\beta_{1-42}$  self-aggregation more efficiently than that of  $A\beta_{1-40}$ , limiting the formation of fibrillar and oligomeric species,<sup>31</sup> and completely blocked the aggregation mediated by AChE of both  $A\beta_{1-42}$  and  $A\beta_{1-40}$ . Interestingly, compound II significantly reduced  $A\beta_{1-42}$ -mediated toxicity in SH-SY5Y human neuroblastoma cells and showed a significant ability to capture free-radical species in vitro as well as a potent effect in preventing the  $A\beta_{1-42}$  induced depletion of catalase and SOD-1.<sup>31,32</sup> Finally, compound II is able to cross the blood–brain barrier in vivo.<sup>33</sup> Overall, these data indicate that hybrid II is the desired *lead* compound in our search for neurodegenerative diseases therapy.

On the basis of these results, we started a *lead compound optimization program*, whose results are described now in this manuscript. From this study, *N*-methyl-*N*-((1-methyl-5-(3-(1-(2-methylbenzyl)piperidin-4-yl)propoxy)-1*H*-indol-2-yl)methyl)prop-2-yn-1-amine (2, MBA236) has emerged as a permeable, potent, irreversible, and quite selective hMAO-A inhibitor (MAOAI) in the nanomolar range, showing also moderate and almost equipotent hAChE vs hBuChE inhibition power.

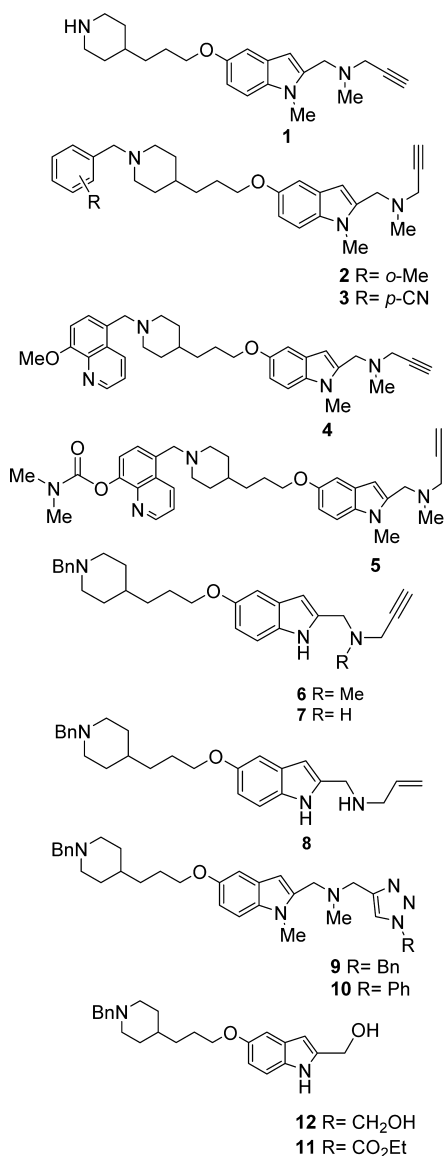
## RESULTS AND DISCUSSION

**Design.** In Figure 1, we show the modifications in compounds I and II which have resulted into the new 19 molecules that we have synthesized. Our selection was based on QSAR analysis (see below) and simple functional changes on compounds II (Figure 2) and I (Figure 3).

As depicted, the *N*-benzyl motif in compound II has been eliminated (1) or modified incorporating different substituents in the phenyl ring, such as *o*-MeC<sub>6</sub>H<sub>5</sub>CH<sub>2</sub> (2), *p*-CNC<sub>6</sub>H<sub>5</sub>CH<sub>2</sub> (3), and *N*-[(8-*O*-methyl- or 8-*O*-(*N,N'*-dimethylcarbamoyl)]5-methylen]quinolone (4 and 5) (Figure 2). Taking into account the structure, inhibition power, and selectivity of compound I for MAO B,<sup>27</sup> the *N*(1)Me in compound II has been replaced by a *N*1(H) leading to 6; the *N*(1)Me and (indole)C(2)-CH<sub>2</sub>N(Me)CH<sub>2</sub>C≡CH in hybrid II has been replaced by a *N*1(H) and (indole)C(2)CH<sub>2</sub>N(H)CH<sub>2</sub>C≡CH in 7 (Figure 2); compound 8 is like 7 (Figure 2), but the acetylene has been substituted by a vinyl group. Compounds 9 and 10 (Figure 2) are the *N*-benzyl- and *N*-phenyl-1,2,3-triazole derivatives,<sup>34</sup> respectively, of compound II. Similarly, compounds 11 and 12 (Figure 2) result from hybrid II by eliminating the C(2)-CH<sub>2</sub>N(Me)CH<sub>2</sub>C≡CH side chain by CH<sub>2</sub>OH, and CO<sub>2</sub>Et,<sup>35</sup> respectively, and in both cases we have replaced the *N*(1)Me group by *N*(1)H.

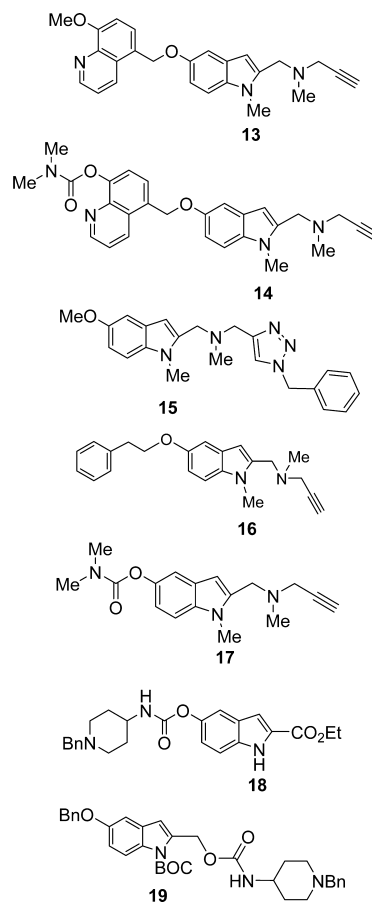
Regarding compound I,<sup>27</sup> related transformations have afforded compounds 13–16 (Figure 3). Compounds 17–19 (Figure 3) are ladostigil/rasagiline-like carbamates, where we wanted to explore the known ability of compounds bearing this functional motif to inhibit ChEs.<sup>36</sup> Results from recent MAO/ChE literature, such as the substitution of an acetylene by a triazole<sup>34</sup> or the use of a multifunctional chelator derived from 8-hydroxyquinoline,<sup>37</sup> have been used to design molecules 5, 9, 10, 14, and 15 (Figures 2 and 3).

**QSAR Analysis.** The 3D-QSAR study has been carried out with main aim to explain and predict the binding on the active sites of human MAO-A, MAO-B, AChE, and BuChE enzymes based on the pharmacological activities<sup>27,31,35</sup> previously observed for the lead-improving program work with multipotent compound II (Supporting Information), and the results are shown in Table 1.



**Figure 2.** Compounds 1–12 synthesized and designed from compound II.

In the data set of previously characterized indole derivatives,<sup>27,31,35</sup> the MAO-A pIC<sub>50</sub> activity interval spanned 4 log units (3.07–9.10); for pIC<sub>50</sub> (MAO-B), it was 5.6 log units (4.00–10.60), for pIC<sub>50</sub> (AChE) 4.2 log units (4.00–8.17), and pIC<sub>50</sub> (BuChE) 3.4 log units (4.00–7.44). The relatively wide pIC<sub>50</sub> interval of the training set provide broad applicability domain for the 3D-QSAR models created. The 3D-QSAR (MAO A) model with two significant components ( $A = 2$ ):  $R^2$ , 0.94; leave-one-out cross validation  $Q^2$ , 0.66; training set parameters ( $R^2_{\text{Observed vs Predicted}}$ , 0.908; and RMSEE, 0.433), and test set parameters ( $R^2_{\text{Observed vs Predicted}}$ , 0.809; and RMSEP, 0.617), was developed. The 3D-QSAR (MAO B) model with two significant components ( $A = 2$ ):  $R^2$ , 0.97; leave-one-out cross validation  $Q^2$ , 0.85; training set parameters ( $R^2_{\text{Observed vs Predicted}}$ , 0.957; and RMSEE, 0.303), and Test set parameters ( $R^2_{\text{Observed vs Predicted}}$ , 0.787; and RMSEP, 0.598) was formed. Similarly, the 3D-QSAR (AChE) model with three significant components ( $A = 3$ ):  $R^2$ , 0.87; leave-one-out cross validation  $Q^2$ , 0.61, training set parameters ( $R^2_{\text{Observed vs Predicted}}$ , 0.873; and RMSEE, 0.431), and test set parameters

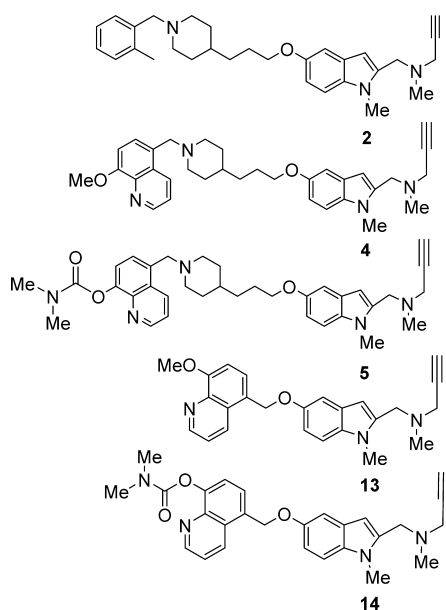


**Figure 3.** Synthesized compounds 13–19 designed from compound I.

( $R^2_{\text{Observed vs Predicted}}$ , 0.539; and RMSEP, 0.661) was developed. The 3D-QSAR (BuChE) model with two significant components ( $A = 2$ ):  $R^2$ , 0.92; leave-one-out cross validation  $Q^2$ , 0.72; training set parameters ( $R^2_{\text{Observed vs Predicted}}$ , 0.922; and RMSEE, 0.261), and test set parameters ( $R^2_{\text{Observed vs Predicted}}$ , 0.657; and RMSEP, 0.521) was created.<sup>35</sup>

The statistical parameters indicated that the 3D-QSAR (MAO-A, MAO-B, AChE, BuChE) models could be used for prediction of MAO-A, MAO-B, AChE, and BuChE inhibiting activities for novel analogues of compounds I and II. Reliability of the activities predictions is strongly related to the type and extent of structural changes of the lead compounds.

3D-pharmacophores are derived from 3D maps of interaction energies between the examined molecule and four chemical probes: DRY (which represent hydrophobic interactions), O ( $sp^2$  carbonyl oxygen, representing H-bond acceptor), N1 (neutral flat NH, like in amide, H-bond donor), and the TIP probe (molecular shape descriptor). The 3D pharmacophores for MAO-A and MAO-B inhibiting activities of compound II contain crucial favorable O-TIP/O-DRY/TIP-TIP/DRY-TIP interactions to the propargylamine moiety and to the benzyl group. Therefore, substitution of the benzyl moiety of hybrid II with small groups, such as an *o*-Me in 2 (Figure 2), could enhance the MAO-A and MAO-B inhibiting activity of the examined compounds by facilitating the TIP-TIP/DRY-TIP favorable interactions. The 3D-QSAR study confirmed also previous experimental findings that the propargylamine moiety provides an essential positive influence on the MAO-A and MAO-B inhibiting activity.<sup>35,38,39</sup>

**Table 1. Experimental and QSAR-Predicted Activities of Novel MAO/ChE Inhibitors**

compd	experimental IC <sub>50</sub> (hMAO-A) <sup>a</sup> (nM)	predicted IC <sub>50</sub> (MAO-A)
2	6.3 ± 0.4	3.9 nM
4	10.3 ± 0.8	218.8 nM
5	257.6 ± 11.4	306.2 nM
14	310.6 ± 17.1	3.2 μM
13	630.1 ± 16.1	23.7 μM
compd	experimental IC <sub>50</sub> (hMAO-B) <sup>a</sup> (nM)	predicted IC <sub>50</sub> (MAO-B)
2	183.6 ± 7.4	100.7 nM
13	164.7 ± 12.1	662.2 nM
5	196.3 ± 7.8	38.8 μM
14	273.1 ± 8.9	58.5 μM
4	7.9 ± 0.5	73.1 μM
compd	experimental IC <sub>50</sub> (hAChE) (μM)	predicted IC <sub>50</sub> (AChE)
2	2.8 ± 0.1	849.2 nM
5	8.4 ± 0.9	3.0 μM
14	<i>b</i>	4.0 μM
4	<i>c</i>	10.3 μM
13	<i>b</i>	11.1 μM
compd	experimental IC <sub>50</sub> (hBuChE) (μM)	predicted IC <sub>50</sub> (BuChE) (μM)
2	4.9 ± 0.2	1.3
5	5.9 ± 0.4	4.4
4	<i>b</i>	9.8
14	<i>b</i>	14.8
13	<i>b</i>	202.8

<sup>a</sup>After 15 min preincubation, so not directly comparable with the predicted IC<sub>50</sub> values. <sup>b</sup>Inactive at 100 μM (highest concentration tested). <sup>c</sup>100 μM inhibits the corresponding MAO activity by approximately 40–50%. At higher concentration the compounds precipitate.

The 3D-pharmacophores for BuChE inhibiting activities of lead compound II contain specific unfavorable TIP-TIP/DRY-TIP interactions between the indole and the *para* position of the benzyl moieties. Therefore, substitution with bulky substituent at *para* position of the benzyl moiety, such as a cyano group in 3 (Figure 2), could decrease BuChE inhibiting activity of compound II derivatives (Table 1). The 3D-pharmacophores for AChE inhibiting activities of compound II contain a crucial favorable O–O interaction to the piperidine

ring and to *ortho* positions of the benzyl group. Thus, a small substituent at *ortho* position of the benzyl ring, such as the methyl group in compound 2 (Figure 2), could enhance AChE inhibiting activity of lead compound II (Table 1).

In addition to 2, compounds 4, 3, 13, and 14 have also been investigated by QSAR analysis, and their predicted IC<sub>50</sub> values are also shown in Table 1. The predicted IC<sub>50</sub> values clearly suggest that (a) compound II-donepezil type hybrids 2, 4, and 5, in this order, should be the most potent MAO-AI, (b) the compound I-like derivative 14 should be a more potent inhibitor of MAO-A, AChE, and BuChE than 13, and (c) 2 should be the most potent inhibitor against all four enzymes.

Next, the designed compound II analogues were synthesized and examined for MAO/ChE inhibitory activity.

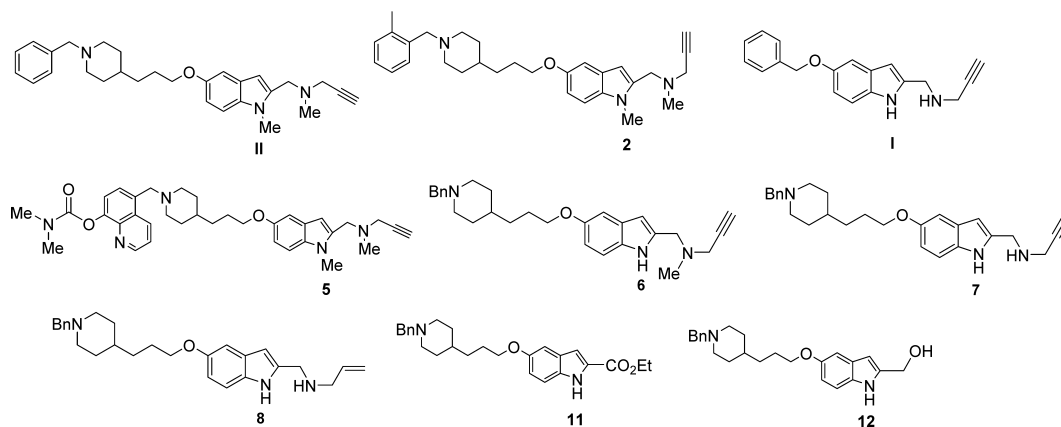
**Chemistry.** The synthesis of the new molecules (Figures 2 and 3) has been achieved by standard or reported methods, in very efficient and short synthetic sequences, in good overall yields (see Supporting Information). All new molecules gave satisfactory analytical and spectroscopic data, in good agreement with their structures.

**Biological Evaluation.** The biological evaluation, comprising the hMAO-A/hMAO-B and hAChE/hBuChE inhibition, has been carried out according to the protocols described in the Supporting Information, following the usual methods.<sup>40,41</sup> In Table 1S (Supporting Information), we have shown the IC<sub>50</sub> values for the inhibition of the MAOs and ChEs with all the 19 new compounds, using compounds I and II, reanalyzed in this work<sup>42</sup> as reference compounds. The established MAOI, clorgyline and L-deprenyl, and the ChEI, donepezil, are also reported for comparative purposes. Note that only seven compounds, 2, 5–8, 11, and 12, were active simultaneously in the four enzymes (Table 2). As shown in Supporting Information, Table 1S, compound 6 is a moderate hMAO-AI and hBuChEI, in the high micromolar range, but shows very modest hMAO-B and hAChE inhibition power. 12 is almost equipotent with 6 for the hMAO-A and hAChE inhibition, but 2.6-fold more, and 4.4-fold less potent than 6, for the inhibition of hMAO-B and hBuChE, respectively. 7 is a poor hMAO-AI and hMAO-BI, but a moderate hAChEI and BuChEI, in the micromolar range. 8 is a quite poor hMAO-AI, hMAO-BI, and hBuChEI but a modest hAChEI. Furthermore, 5 and 11 were nonselective, potent hMAOI in the low micromolar range, but moderate and equipotent ChE inhibitors.

However, among all these products, as predicted by the QSAR analysis (see above), compound 2 (Table 2) was the most potent hMAO-A, hMAO-B AChE, and BuChE multipotent inhibitor found in this work. Compound 2 is a very potent, in the nanomolar range, and selective hMAO-AI ( $K_i = 7.5 \pm 0.9$  nM), showing a potent and slightly selective hAChE inhibition profile ( $K_i = 1.3 \pm 0.5$  μM), in the micromolar range. Compared with the reference compound II (Figure 4), the new compound 2 is 9.2-fold and 6.5-fold more potent hMAO-AI and hMAO-BI, respectively, 1.2-fold more potent hAChEI, and only 1.5-fold less potent hBuChEI. Comparing with compound I and the standard MAOIs, for the inhibition of MAO-A, compound 2 is 45-fold more potent than compound I, 1.3-fold less than clorgyline, and 10095-fold more potent than L-deprenyl. Conversely, for the inhibition of MAO-B, compound 2 is 45-fold less, 358-fold more, and 10-fold less potent than compound I, clorgyline, and L-deprenyl, respectively.

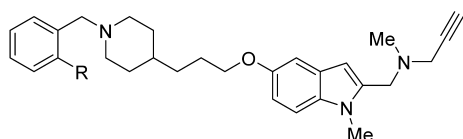
To sum up, compound 2 is a multipotent molecule of MAO and ChE, showing a very attractive pharmacological profile, as a selective and very potent MAO-AI, with high MAO-B and

**Table 2.** IC<sub>50</sub> Values for the Inhibitory Effects of Test Compounds on the Enzymatic Activity for Human MAO or ChE Isoforms and Selectivity Ratios for MAO-B [IC<sub>50</sub> (MAO-A)]/[IC<sub>50</sub> (MAO-B)] or for AChE ([IC<sub>50</sub> (AChE)]/[IC<sub>50</sub> (BuChE)]<sup>a</sup>



compd	hMAO-A	hMAO-B	ratio	hAChE ( $\mu$ M)	hBuChE ( $\mu$ M)	ratio
2	6.3 $\pm$ 0.4 nM <sup>b</sup>	183.6 $\pm$ 7.4 nM	0.03	2.8 $\pm$ 0.1	4.9 $\pm$ 0.2	0.57
5	257.6 $\pm$ 11.4 nM <sup>c</sup>	196.3 $\pm$ 7.8 nM	1.3	8.4 $\pm$ 0.9	5.9 $\pm$ 0.4	1.4
6	9.1 $\pm$ 0.7 $\mu$ M <sup>c</sup>	35.1 $\pm$ 2.8 $\mu$ M	0.26	15.4 $\pm$ 0.9	7.1 $\pm$ 0.5	2.2
7	19.2 $\pm$ 1.3 $\mu$ M <sup>c</sup>	33.6 $\pm$ 1.5 $\mu$ M	0.57	4.9 $\pm$ 0.3	7.3 $\pm$ 0.8	0.67
8	45.3 $\pm$ 1.6 $\mu$ M <sup>c</sup>	21.3 $\pm$ 1.9 $\mu$ M	2.1	4.6 $\pm$ 0.3	40.6 $\pm$ 2.2	0.11
11	876.6 $\pm$ 25.2 nM	1.0 $\pm$ 0.02 $\mu$ M	0.87	9.6 $\pm$ 0.08	9.7 $\pm$ 0.7	0.99
12	9.1 $\pm$ 0.3 $\mu$ M	13.5 $\pm$ 1.1 $\mu$ M	0.67	13.6 $\pm$ 1.4	31.2 $\pm$ 3.1	0.43
II	58.2 $\pm$ 1.2 nM <sup>b</sup>	1.2 $\pm$ 0.1 $\mu$ M	0.05	3.4 $\pm$ 0.2	3.3 $\pm$ 0.2	1.03
I	287.3 $\pm$ 11.2 nM <sup>b</sup>	4.1 $\pm$ 0.7 nM	70	e	e	
clorgyline	4.7 $\pm$ 0.2 nM <sup>b</sup>	65.8 $\pm$ 1.6 $\mu$ M	0.000071	e	e	
L-deprenyl	63.6 $\pm$ 1.3 $\mu$ M <sup>b</sup>	18.2 $\pm$ 0.9 nM	3494	e	e	
donepezil <sup>d</sup>	nd	nd		0.016 $\pm$ 0.001	8.2 $\pm$ 0.2	

<sup>a</sup>All IC<sub>50</sub> values shown in this table are the mean  $\pm$  SD from five experiments. **hMAO:** IC<sub>50</sub> values were determined after 15 min preincubation of inhibitor with the enzyme. **hChE:** IC<sub>50</sub> values were determined after 10 min preincubation of inhibitor with the enzyme. Level of statistical significance: <sup>b</sup>*P* < 0.01 or <sup>c</sup>*P* < 0.05 versus the corresponding IC<sub>50</sub> values obtained against MAO-B, as determined by ANOVA/Dunnett's. <sup>d</sup>Reference 23. <sup>e</sup>Inactive at 100  $\mu$ M (highest concentration tested). nd = not determined.



2 (MBA236) (R= Me)	II (ASS234) (R= H)
IC <sub>50</sub> (hMAO-A): 6.3 $\pm$ 0.4 nM	58.2 $\pm$ 1.2 nM
IC <sub>50</sub> (hMAO-B): 183.6 $\pm$ 7.4 nM	1.2 $\pm$ 0.1 $\mu$ M
IC <sub>50</sub> (hAChE): 2.8 $\pm$ 0.1 $\mu$ M	3.4 $\pm$ 0.2 $\mu$ M
IC <sub>50</sub> (hBuChE): 4.9 $\pm$ 0.2 $\mu$ M	3.3 $\pm$ 0.2 $\mu$ M

**Figure 4.** Structure of compound 2 and its IC<sub>50</sub> values for the inhibition of MAO and ChEs compared with the reference compound II.

potent hAChE/hBuChE inhibition power. It must be also concluded that all our present and past efforts<sup>29</sup> to transform compound I into a multipotent MAO/ChE compound, by transforming the benzyl group into the ChE donepezil-like pharmacophore, have met with success but at the cost of losing significant MAO-B inhibition capacity.

Taking into account these findings, we have performed further studies on the inhibition mechanism of action of compound 2.

Figures 5 and 6 show the results of the reversibility test<sup>43</sup> on hMAO. Compound 2 binds as an irreversible inhibitor on both

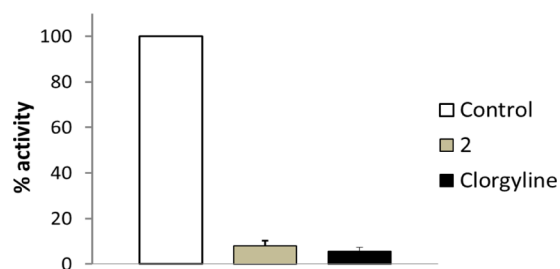


**Figure 5.** Recovery of hMAO-A activity after dilution following incubation (30 min at room temperature) of the 100 $\times$  enzyme concentration with 10-fold IC<sub>50</sub> concentration of compound 2 or clorgyline. The control was carried out by preincubating in the absence of inhibitor and diluting in the same way. Results are expressed as percentage of control. Represented data are mean  $\pm$  SD of five independent assays.

enzyme isoforms, maintaining near a 90% inhibition after the dilution of the preincubated mixture. The IC<sub>50</sub> decreased from 14.6  $\pm$  1.2 nM in reversible conditions (no preincubation and substrate concentration 2  $\times$  K<sub>m</sub>) to 6.3  $\pm$  0.4 nM assayed with saturating substrate after a 15 min incubation.

Nevertheless, the recovery of ChE activity after compound 2 on ChEs was significantly greater (around 20%), allowing us to

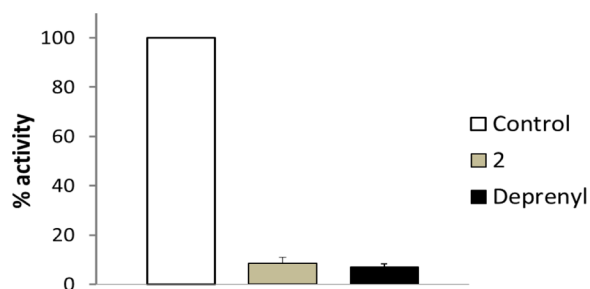


**Figure 6.** Recovery of hMAO-B activity after dilution following incubation (30 min at room temperature) of the 100 $\times$  enzyme concentration with 10-fold  $IC_{50}$  concentration of compound 2 or L-deprenyl. The control was carried out by preincubating in the absence of inhibitor and diluting in the same way. Results are expressed as percentage of control. Represented data are mean  $\pm$  SD of five independent assays.

classify it as a slow inhibitor (Figure 7). Kinetic assays performed with this compound have shown ambiguous results,

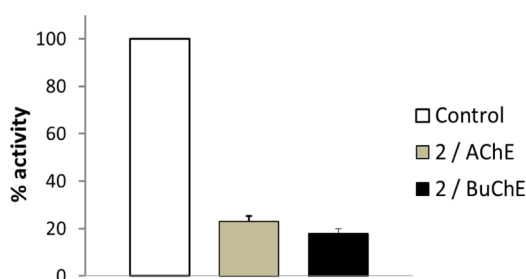


**Figure 7.** Recovery of hAChE (gray column) and hBuChE (black column) activity after the dilution of the incubation (30 min at room temperature) of the 100 $\times$  enzyme concentration and 10-fold  $IC_{50}$  of compound 2. The control was carried out by preincubating in the absence of inhibitor and diluting in the same way. Results are expressed as percentage of control. Represented data are mean  $\pm$  SD of five independent assays.

probably due to the low degree of reversibility of inhibition achieved on hAChE and hBuChE. As a result of the low reversibility, the pattern of the Lineweaver–Burk representation appears to indicate a mixed model for both enzymes (results not shown).

With the aim of investigating compound 2 recognition with respect to either MAO-A, MAO-B, AChE, and BuChE enzymes, molecular modeling studies have been carried out. The theoretical investigation has been focused on the ligand–enzyme interaction and target structural perturbation produced by compound 2 comparing these information with respect to the same data coming from the related compound II (Supporting Information). Only one proposed structure was found for compound 2 in hMAO-A and two for hMAO-B, with a global minimum population equal to 96.11%. Compounds II and 2 both adopted bent conformations in hMAO-A but were linear in hMAO-B (Figure S1, Supporting Information). Overall, the interactions between compounds II, 2, and the MAOs are driven by both steric hindrance and hydrophobic contribution with an additional electrostatic term present in hMAO-A. Using the target RMSd matrix, each MD trajectory was clustered into nine groups. The visual inspection of the 10 structures for each inhibitor with each enzyme clearly indicates the conformation stabilizing effect of the *o*-methyl group in hybrid 2 (Figure S4, Supporting Information).

In this work, we have designed a new and multipotent MAOI. MAOI are well-known for showing diverse therapeutic potential as the result of combining selectivity and (ir)reversible modes of binding.<sup>15</sup> MAO-AI have been used mostly in the treatment of depression and anxiety,<sup>44</sup> and MAO-BI for the treatment of PD.<sup>45</sup> Recent studies have shown that MAO-A is involved in the regulation of serotonin for ventricular remodeling via activation of the serotonin2A receptors.<sup>46</sup> In the aged heart, the increased MAO-A concentrations results in high levels of oxygen peroxide, leading to severe cardiomyocyte damage.<sup>47</sup> A survey of the current literature on MAOIs shows also that one of the major reasons for designing new and specific inhibitors is to function as cardioprotectants for the age-dependent increase of MAO A in the heart.<sup>48</sup> Although MAO-AIs enhance extracellular levels of dopamine produced from L-dopa, irreversible and selective MAO-AI cannot be used in the PD therapy because of cardiovascular side effects.<sup>49</sup> Another disadvantage of an irreversible MAO-AI is the hypertensive “cheese effect”<sup>50</sup> due to the predominance of MAO-A in the gut wall to metabolize tyramine in fermented foods such as cheese and beer. Hypertensive crises may be prevented by using reversible rather than irreversible MAO-AI or tissue-specific inhibitors such as the brain-selective ladostigil.<sup>51</sup>

The cases of ladostigil<sup>52</sup> and M30D<sup>53</sup> (Figure 8) are of interest for this project and future possible endeavors because

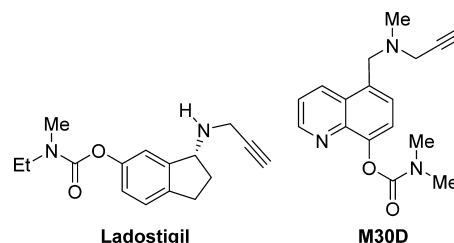


**Figure 8.** Structures of ladostigil and M30D.

both are ChE, MAO-A, and MAO-B irreversible inhibitors with potential therapeutic applications as antidepressants, antiparkinson, and anti-Alzheimer drugs.<sup>44</sup> Ladostigil<sup>51</sup> (Figure 8) was designed from rasagiline, a MAO-BI, bearing a propargylamine motif, responsible for the neuroprotective properties, and a carbamate group, affording ChE inhibitory activity. M30D<sup>53</sup> (Figure 8) shows an inhibitory profile against ChE (hAChE  $IC_{50} = 0.52 \pm 0.07 \mu\text{M}$ ; hBuChE  $IC_{50} = 44.90 \pm 6.10 \mu\text{M}$ ) and against MAO (ratMAO-A,  $IC_{50} = 0.0077 \pm 0.0007 \mu\text{M}$ ; ratMAO-B,  $IC_{50} = 7.90 \pm 1.34 \mu\text{M}$ ) very similar to the one observed for 2 (Table 2), as well as other properties as potential drugs for treating AD.

**In Vitro Blood–Brain Barrier Permeation Assay.** Finally, to evaluate the brain penetration, we used the PAMPA–BBB method described by Di,<sup>54</sup> and subsequently optimized by Rodríguez-Franco et al. for molecules with limited water-solubility.<sup>55–57</sup>

The *in vitro* permeability ( $P_e$ ) value of compound 2 through a lipid extract of porcine brain was determined by using PBS:ethanol (70:30). In the same assay, 11 commercial drugs of known CNS penetration were also tested and their experimental values were compared to reported values, giving a good lineal correlation,  $P_e(\text{exp}) = 1.4442 P_e(\text{bibl}) + 6.5263$  ( $R^2 = 0.95$ ). From this equation and taking account the limits established by Di for BBB permeation,<sup>54</sup> we found that

compounds with permeability values above  $12.3 \times 10^{-6} \text{ cm s}^{-1}$  could penetrate into the CNS. Derivative **2** showed  $P_e = 14.4 \pm 0.4 \times 10^{-6} \text{ cm s}^{-1}$ , and thus, it could cross BBB by passive diffusion (Supporting Information).

## CONCLUSIONS

In this paper, we have reported the design, synthesis, and biological evaluation of 19 new donepezil–indolyl hybrids as multifunctional drugs able to bind MAO and ChE enzymes, using the MAO B inhibitor **I** hit and the multipotent **II** hybrid lead as references for lead-optimization in order to discover a new lead compound for deeper in vivo preclinical investigations targeted to neurological disorders. The QSAR-designed compound **II** analogues have been synthesized and examined for MAO/ChE inhibitory activity. As shown in Figure 4, the potent MAO/ChE inhibiting activity for the novel ligand **2** confirmed the quality of the optimized 3D-pharmacophores for use in future work to design novel donepezil–indolyl hybrids. We have found significant biological activity on the four enzymes studied in almost half of the synthesized structures. The most promising compound of the series, **2**, acted as an irreversible hMAO-AI, potent in the nanomolar range, nine times more potent than the reference compound **II**, and 29-fold more selective for hMAO-A over hMAO-B. Inhibition of the ChEs by hybrid **2** is in the micromolar range, slightly better than compound **II** for hAChEs although slightly poorer for hBuChE. Although we are confronted with unbalanced, highly preferred MAO vs ChE inhibition, the potency and desired balance between targets in MTDL-based strategies is not known.<sup>58</sup> Molecular modeling studies<sup>59</sup> reported similar binding modes of compounds **II** and **2** in all the evaluated biological targets. The *o*-Me group in compound **2** improves the ligand recognition, increasing the ligand–enzyme hydrophobic interaction in hBuChE and  $\pi$ – $\pi$  stacking in hMAO-A, hMAO-B, and hAChE. Thus, it is clear that simple modification of compound **II**, such as the incorporation of an *o*-methyl instead of a hydrogen in the phenyl ring of the *N*-benzylpiperidine motif, produces significant qualitative and quantitative pharmacological changes in the inhibition of MAO and ChE enzymes. Finally, the ADMET virtual analysis<sup>59</sup> suggests that inhibitor **2** should present good drug-like characteristics similar to compound **II**, with a slightly better brain penetration ability, a prediction experimentally confirmed by the in vitro blood–brain barrier permeation assay.

Consequently, we have fulfilled our initial expectations, that a new, easily available, permeable multipotent MAO inhibitor has been discovered. The related pharmacological properties with ladostigil, clearly support projected in vivo studies for proof of concept targeted to probe the suitability of compounds **2** and **II** to treat neurodegenerative disorders such AD or PD.

## ASSOCIATED CONTENT

### Supporting Information

QSAR methods, ADMET analysis and descriptors, the synthesis of the target compounds, the <sup>1</sup>H and <sup>13</sup>C spectra, biological evaluation, molecular modeling, and in vitro blood–brain barrier permeation assay of compound **2**. This material is available free of charge via the Internet at <http://pubs.acs.org>.

## AUTHOR INFORMATION

### Corresponding Authors

\*For J.M.-C.: phone, +34-91-5622900; fax, +34-91-5644853; E-mail, [iqoc21@iqoc.csic.es](mailto:iqoc21@iqoc.csic.es).

\*For M.Y.: phone, +34-881-815529; fax, +34-881-545595; E-mail, [matilde.yannez@uam.es](mailto:matilde.yannez@uam.es).

\*For F.O.: phone, +39-09613694197; fax, +39 0961391490; E-mail, [ortuso@unicz.it](mailto:ortuso@unicz.it).

## Author Contributions

O.M.B.A. carried out the synthesis of the target molecules. O.M.B.A., M.C., and A.S. carried out the spectroscopic analyses. K.N., S.F., and D.A. carried out the QSAR predictions. M.Y. undertook the enzyme inhibition and mechanistic studies. E.S. did the ADMET-analysis. F.O. and S.A. carried out the computational studies. L.d.A. did the PAMPA–BBB experiment, under M.I.R.-F. supervision. R.R.R. evaluated the data and contributed to writing the manuscript. J.M.-C. conceived, designed, and supervised the project.

## Notes

The authors declare no competing financial interest.

## ACKNOWLEDGMENTS

J.M.-C. thanks MINECO (Spain) for grant SAF2012-33304, and Universidad Camilo José Cela (Madrid, Spain) for support (MULTIMOL 2013-20). Oscar Mauricio Bautista-Aguilera thanks MINECO for a FPI fellowship. This work was supported by the COST action CM1103. D.A., K.N., and S.F. acknowledge COST action CM1207 and the project (contract no. 172033) supported by the Ministry of Education and Science of the Republic of Serbia. M.I.R.-F. acknowledges the financial support from the Spanish Ministry of Economy and Competitiveness (SAF2012-31035), CSIC (PIE-201280E074), and Fundación de Investigación Médica Mutua Madrileña Automovilística (AP103952012).

## ABBREVIATIONS USED

ACh, acetylcholine; AChEI, acetylcholinesterase inhibitors; hAChE, human acetylcholinesterase; AD, Alzheimer's disease; ADMET, absorption, distribution, metabolism, excretion, toxicity; hBuChE, human butyrylcholinesterase; hERG, human *ether-à-go-go*-related gene; MAO, monoamine oxidase-A/B; MAOI, monoamine oxidase inhibitors; MTDL, multi-target-directed ligand; PAMPA–BBB, parallel artificial membrane permeation assay/blood–brain barrier; QSAR, quantitative structure–activity relationships

## REFERENCES

- (1) Castellani, R. J.; Rolston, R. K.; Smith, M. A. Alzheimer disease. *Dis. Month* **2010**, *56*, 484–546.
- (2) Reitz, C.; Brayne, C.; Mayeux, R. Epidemiology of Alzheimer disease. *Nature Rev. Neurol.* **2011**, *7*, 137–152.
- (3) Goedert, M.; Spillantini, M. G. A century of Alzheimer's disease. *Science* **2006**, *314*, 777–781.
- (4) Terry, R. D.; Gonatas, N. K.; Weiss, M. Ultrastructural studies in Alzheimer's presenile dementia. *Ann. J. Pathol.* **1964**, *44*, 269–297.
- (5) Grundke-Iqbal, I.; Iqbal, K.; Tung, Y. C.; Quinlan, M.; Wisniewski, H. M.; Binder, L.I. Abnormal phosphorylation of the microtubule-associated protein  $\tau$  (tau) in Alzheimer cytoskeletal pathology. *Proc. Natl. Acad. Sci. U. S. A.* **1986**, *93*, 4913–4917.
- (6) Rosini, M.; Simoni, E.; Milelli, A.; Minarini, A.; Melchiorre, C. Oxidative stress in Alzheimer's disease: Are we connecting the dots? *J. Med. Chem.* **2014**, *57*, 2821–2831.
- (7) Perry, E. K.; Tomlinson, B. E.; Blesseed, G.; Bergmann, K.; Gibson, P. H.; Perry, R. H. Correlation of cholinergic abnormalities with senile plaques and mental test scores in senile dementia. *Br. Med. J.* **1978**, *2*, 1457–1459.
- (8) Talsma, V. N. Acetylcholinesterase in Alzheimer's disease. *Mech. Ageing Dev.* **2001**, *122*, 1961–1969.

- (9) Terry, A. V.; Buccafusco, J. J.; Wilson, C. Cognitive dysfunction in neuropsychiatric disorders: selected serotonin receptor subtypes as therapeutic targets. *Behav. Brain Res.* **2008**, *195*, 30–38.
- (10) Youdim, M. B. H.; Finberg, J. P. M.; Tipton, K. F. Monoamine oxidase. In *Handbook of Experimental Pharmacology*; Tredelenburg, U., Weiner, N., Eds.; Springer-Verlag: Berlin, 1988; Vol. 20, pp 119–192.
- (11) Johnston, J. P. Some observations upon a new inhibitor of monoamine oxidase in brain tissue. *Biochem. Pharmacol.* **1968**, *17*, 1285–1297.
- (12) Grimsby, J.; Lan, N. C.; Neve, R.; Chen, K.; Shih, J. C. Tissue distribution of human monoamine oxidase A and B mRNA. *J. Neurochem.* **1990**, *55*, 1166–1169.
- (13) Harfenist, H.; Heuseur, D. J.; Joyner, C. T.; Batchelor, J. F.; White, H. L. Selective inhibitors of monoamine oxidase. 3. Structure–activity relationship of tricyclics bearing imidazoline, oxadiazole, or tetrazole groups. *J. Med. Chem.* **1996**, *39*, 1857–1863.
- (14) Riederer, P.; Danielczyk, W.; Grünblatt, E. Monoamine oxidase-B inhibition in Alzheimer's disease. *Neurotoxicology* **2004**, *25*, 271–277.
- (15) Finberg, J. P. M. Update on the pharmacology of selective inhibitors of MAO-A and MAO-B: focus on modulation of CNS neurotransmitters. *Pharmacol. Ther.* **2014**, *143*, 133–152.
- (16) Gura, T. Hope in Alzheimer's fight emerges from unexpected places. *Nature Med.* **2008**, *14*, 894.
- (17) Racchi, M.; Mazzucchelli, M.; Porrello, E.; Lanni, C.; Govoni, S. Acetylcholinesterase inhibitors: novel activities of old molecules. *Pharmacol. Res.* **2004**, *50*, 441–451.
- (18) Muñoz-Torrero, D. Acetylcholinesterase inhibitors as disease-modifying therapies for Alzheimer's disease. *Curr. Med. Chem.* **2008**, *15*, 2433–2455.
- (19) Castro, A.; Martínez, A. Targeting beta-amyloid pathogenesis through acetylcholinesterase inhibitors. *Curr. Pharm. Des.* **2006**, *12*, 4377–4387.
- (20) Cavalli, A.; Bolognesi, M. L.; Minarini, A.; Rosini, M.; Tumiatti, V.; Recanatini, M.; Melchiorre, C. Multi-target-directed ligands to combat neurodegenerative diseases. *J. Med. Chem.* **2008**, *51*, 347–372.
- (21) León, R.; García, A. G.; Marco-Contelles, J. Recent advances in the multitarget-directed ligands approach for the treatment of Alzheimer's disease. *Med. Res. Rev.* **2013**, *33*, 139–189.
- (22) Anighoro, A.; Bajorath, J.; Rastelli, G. Polypharmacology: challenges and opportunities in drug discovery. *J. Med. Chem.* **2014**, *57*, 7874–7887.
- (23) Rosini, M.; Antonello, A.; Cavalli, A.; Bolognesi, M. L.; Minarini, A.; Marucci, G.; Poggesi, E.; Leonardi, A.; Melchiorre, C. Prazosin-related compounds. Effect of transforming the piperazinylnazoline moiety into an aminomethyltetrahydroacridine system on the affinity for  $\alpha_1$ -adrenoreceptors. *J. Med. Chem.* **2003**, *46*, 4895–4903.
- (24) Fang, L.; Appenroth, D.; Decker, M.; Kiehltopf, M.; Roegler, C.; Deufel, T.; Fleck, C.; Peng, S.; Zhang, Y.; Lehmann, J. Synthesis and biological evaluation of NO-donor–tacrine hybrids as hepatoprotective anti-Alzheimer drug candidates. *J. Med. Chem.* **2008**, *51*, 713–716.
- (25) Stosel, A.; Schlenk, M.; Hinz, S.; Kuppers, P.; Heer, J.; Gutschow, M.; Müller, C. E. Dual targeting of adenosine A2A receptors and monoamine oxidase B by 4H-3,1-benzothiazin-4-ones. *J. Med. Chem.* **2013**, *56*, 4580–4596.
- (26) Fang, L.; Kraus, B.; Lehmann, J.; Heilmann, J.; Zhang, Y.; Decker, M. Design and synthesis of tacrine–ferulic acid hybrids as multi-potent anti-Alzheimer drug candidates. *Bioorg. Med. Lett.* **2008**, *18*, 2905–2909.
- (27) V. Pérez, V.; Marco, J. L.; Fernández-Álvarez, E.; Unzeta, M. Relevance of benzyloxy group in 2-indolyl methylamines in the selective MAO-B inhibition. *Br. J. Pharmacol.* **1999**, *127*, 869–876.
- (28) Bolea, I.; Gella, A.; Unzeta, M. Propargylamine-derived multitarget-directed ligands: fighting Alzheimer's disease with monoamine oxidase inhibitors. *J. Neural. Transm.* **2013**, *120*, 893–902.
- (29) Bolea, I.; Juárez-Jiménez, J.; de los Ríos, C.; Chioua, M.; Pouplana, R.; Luque, F. J.; Unzeta, M.; Marco-Contelles, J.; Samadi, A. Synthesis, biological evaluation, and molecular modeling of donepezil and *N*-[(5-(benzyloxy)-1-methyl-1*H*-indol-2-yl)methyl]-*N*-methylprop-2-yn-1-amine hybrids as new multipotent cholinesterase/monoamine oxidase inhibitors for the treatment of Alzheimer's Disease. *J. Med. Chem.* **2011**, *54*, 8251–8270.
- (30) Esteban, G.; Allan, J.; Samadi, A.; Mattevi, A.; Unzeta, M.; Marco-Contelles, J.; Binda, C.; Ramsay, R. R. Kinetic and structural analysis of the irreversible inhibition of human monoamine oxidases by ASS234 a multi-target compound for designed for use in Alzheimer's disease. *Biochim. Biophys. Acta, Proteins Proteomics* **2014**, *1844*, 1104–1110.
- (31) Bolea, I.; Gella, A.; Monjas, L.; Pérez, C.; Rodríguez-Franco, M. I.; Marco-Contelles, J. L.; Samadi, A.; Unzeta, M. The multipotent, permeable drug ASS234 inhibits A $\beta$  aggregation, possesses antioxidant properties and protects from A $\beta$ -induced apoptosis. *Curr. Alzheimer Res.* **2013**, *9*, 797–808.
- (32) del Pino, J.; Ramos, E.; Bautista Aguilera, O. M.; Marco-Contelles, J.; Romero, A. Wnt signaling pathway, a potential target for Alzheimer's disease treatment, is activated by a novel multitarget compound ASS234. *CNS Neurosci. Ther.* **2014**, *20*, 568–570.
- (33) Stasiak, A.; Mussur, M.; Unzeta, M.; Samadi, A.; Marco-Contelles, J. L.; Fogel, W. A. Effects of novel monoamine oxidases and cholinesterases targeting compounds on brain neurotransmitters and behavior in rat model of vascular dementia. *Curr. Pharm. Des.* **2014**, *20*, 161–171.
- (34) Zhu, Z. J. 'Clik' assembly of selective inhibitors of MAO-A. *Bioorg. Med. Chem. Lett.* **2010**, *20*, 6222–6225.
- (35) Bautista-Aguilera, O. M.; Esteban, G.; Bolea, I.; Nikolic, K.; Agbaba, D.; Moraleda, I.; Iriepa, I.; Samadi, A.; Soriano, E.; Unzeta, M.; Marco-Contelles, J. Design, synthesis, pharmacological evaluation, QSAR analysis, molecular modeling and ADMET of novel donepezil–indolyl hybrids as multipotent cholinesterase/monoamine oxidase inhibitors for the potential treatment of Alzheimer's disease. *Eur. J. Med. Chem.* **2014**, *75*, 82–95.
- (36) Sterling, J.; Herzig, Y.; Goren, T.; Finkelstein, N.; Lerner, D.; Goldenberg, W.; Mikolczi, I.; Molnar, S.; Rantal, F.; Tamas, T.; Toth, G.; Zagvyva, A.; Zekany, A.; Finberg, J.; Lavian, G.; Gross, A.; Friedman, R.; Razin, M.; Huang, W.; Kraus, B.; Chorev, M.; Youdim, M. B.; Weinstock, M. Novel dual inhibitors of AChE and MAO derived from hydroxyl aminoindan and phenethylamine as potential treatment for Alzheimer's disease. *J. Med. Chem.* **2002**, *54*, 5260–5279.
- (37) Zheng, H.; Youdim, M. B. H.; Fridkin, M. Site-activated multifunctional chelator with acetylcholinesterase and neuroprotective-neurorestorative moieties for Alzheimer's disease. *J. Med. Chem.* **2009**, *52*, 4095–4098.
- (38) Yogeve-Falach, M.; Bar-Am, O.; Amit, T.; Weinreb, O.; Youdim, M. B. A multifunctional, neuroprotective drug, ladostigil (TV3326), regulates holo-APP translation and processing. *FASEB J.* **2006**, *20*, 2177–2179.
- (39) Youdim, M. B.; Weinstock, M. Molecular basis of neuroprotective activities of rasagiline and the anti-Alzheimer drug TV3326. *Cell. Mol. Neurobiol.* **2002**, *21*, 555–573.
- (40) Ellman, G. L.; Courtney, K. D.; Andres, B. J.; Featherstone, R. M. A new and rapid colorimetric determination of acetylcholinesterase activity. *Biochem. Pharmacol.* **1961**, *7*, 88.
- (41) Yáñez, M.; Fraiz, N.; Cano, E.; Orallo, F. Inhibitory effects of *cis*- and *trans*-resveratrol on noradrenaline and 5-hydroxytryptamine uptake and on monoamine oxidase activity. *Biochem. Biophys. Res. Commun.* **2006**, *344*, 688–695.
- (42) Reevaluation of reference inhibitors has been carried out under different conditions (enzymatic source and concentrations, measurement method) than our previous study (refs 29 and 30, cited herein) but finding similar qualitative inhibition and selectivity for all compounds tested. Because IC<sub>50</sub> values depends directly on enzyme and substrate concentrations, normal quantitative discrepancies were achieved.
- (43) Copeland, R. A. *Evaluation of Enzyme Inhibitors in Drug Discovery*; Wiley-Interscience: Hoboken, NJ, 2005.

(44) Youdim, B. H. M.; Edmondson, D.; Tipton, K. F. The therapeutic potential of monoamine oxidase inhibitors. *Nature Rev. Neurosci.* **2006**, *7*, 295–309.

(45) Palhagen, S.; Heinonen, E.; Hagglund, J.; Kaugesaar, T.; Maki-Ikola, O.; Palm, R. Selegiline slows the progression of the symptoms of Parkinson disease. *Neurology* **2006**, *66*, 1200–1206.

(46) Lairez, O.; Calise, D.; Bianchi, P.; Ordener, C.; Spreux-Varoquaux, O.; Guilbeau-Frugier, C.; Escourrou, G.; Seif, I.; Roncalli, J.; Pizzinat, N.; Galinier, M.; Parini, A.; Mialet-Pérez, J. Genetic deletion of MAO-A promotes serotonin-dependent ventricular hypertrophy by pressure overload. *J. Mol. Cell Cardiol.* **2009**, *46*, 587–95.

(47) Di Lisa, F.; Kaludercic, N.; Carpi, A.; Menabo, R.; Giogio, M. Mitochondrial pathways for ROS formation and myocardial injury: The relevance of p66Shc and monoamine oxidase. *Basic Res. Cardiol.* **2009**, *104*, 131–139.

(48) Edmondson, D. E. Hydrogen peroxide produced by mitochondrial monoamine oxidase catalysis: biological implications. *Curr. Pharm. Des.* **2014**, *20*, 155–160.

(49) Finberg, J. P.; Gross, A.; Bar-Am, O.; Friedman, R.; Loboda, Y.; Youdim, M. B. Cardiovascular responses to combined treatment with selective monoamine oxidase type B inhibitors and L-DOPA in the rat. *Br. J. Pharmacol.* **2006**, *149*, 647–656.

(50) Finberg, J. P.; Gillman, P. K. Selective inhibitors of monoamine oxidase Type B and the “cheese effect”. In *International Review of Neurobiology*; Youdim, M. B., Riederer, P., Eds.; Academic Press: Burlington, 2011; Vol. 100, pp 169–190.

(51) Weinstock, M.; Gorodetsky, E.; Wang, R. H.; Gross, A.; Weinreb, O.; Youdim, M. B. Limited potentiation of blood pressure response to oral tyramine by brain-selective monoamine oxidase A-B inhibitor, TV-3326 in conscious rabbits. *Neuropharmacology* **2002**, *43*, 999–1005.

(52) Yogev-Falach, M.; Bar-Am, O.; Amit, T.; Weinreb, O.; Youdim, M. B. H. A multifunctional, neuroprotective drug, ladostigil (TV3326), regulates holo-APP translation and processing. *FASEB J.* **2006**, *20*, 2177–2179.

(53) Zheng, H.; Fridkin, M.; Youdim, M. B. H. Site-activated chelators derived from anti-Parkinson drug rasagiline as a potential safer and more effective approach to the treatment of Alzheimer’s disease. *Neurochem. Res.* **2010**, *35*, 2117–2123.

(54) Di, L.; Kerns, E. H.; Fan, K.; McConnell, O. J.; Carter, G. T. High throughput artificial membrane permeability assay for blood–brain barrier. *Eur. J. Med. Chem.* **2003**, *38*, 223–232.

(55) Rodríguez-Franco, M. I.; Fernández-Bachiller, M. I.; Pérez, C.; Hernández-Ledesma, B.; Bartolomé, B. Novel tacrine–melatonin hybrids as dual-acting drugs for Alzheimer disease, with improved acetylcholinesterase inhibitory and antioxidant properties. *J. Med. Chem.* **2006**, *49*, 459–462.

(56) Fernández-Bachiller, M. I.; Pérez, C.; Monjas, L.; Rademann, J.; Rodríguez-Franco, M. I. New tacrine-4-oxo-4H-chromene hybrids as multifunctional agents for the treatment of Alzheimer’s disease, with cholinergic, antioxidant, and beta-amyloid-reducing properties. *J. Med. Chem.* **2012**, *55*, 1303–1317.

(57) López-Iglesias, B.; Pérez, C.; Morales-García, J. A.; Alonso-Gil, S.; Pérez-Castillo, A.; Romero, A.; López, M. G.; Villarroya, M.; Conde, S.; Rodríguez-Franco, M. I. New melatonin-*N,N*-dibenzyl(*N*-methyl)amine hybrids: potent neurogenic agents with antioxidant, cholinergic, and neuroprotective properties as innovative drugs for Alzheimer’s disease. *J. Med. Chem.* **2014**, *57*, 3773–3785.

(58) Prati, F.; Uliassib, E.; Bolognesi, M. L. Two diseases, one approach: multitarget drug discovery in Alzheimer’s and neglected tropical diseases. *Med. Chem. Commun.* **2014**, *5*, 853–861.

(59) ADMET and molecular modeling details and results have been reported in the Supporting Information.